



Numerical Prediction of Free Convection Phenomena Through a Rectangular Inclined Cavity Filled with a Porous Media.

By:

Dr. Ahmed Kadhim Hussein

Lecturer - College of Engineering-Mechanical Engineering Department
Babylon University- Babylon City – Hilla – IRAQ.
e-mail ahmedkadhim74@yahoo.com

1. Abstract:

Numerical simulation of free convection air flow through a porous media in an inclined rectangular cavity is studied. Physical problem consists of a rectangular inclined cavity filled with a porous media. The top and bottom surfaces are thermally insulated while the left and right walls are maintained at isothermal hot and cold temperatures respectively. The two-dimensional flow is characterized using Under-Relaxation finite difference scheme. It is found that the two-dimensional flow is characterized by the vortices that are initiated by the existence of buoyancy effect. The problem considered deals with a two-dimensional internal, laminar, isothermal flow in an inclined rectangular porous cavity. In this work, the Darcy model is used and the governing equations are solved using Under-Relaxation explicit technique for flow characteristics of Prandtl number at 0.7, an aspect ratio equals to 1.5, Rayleigh number ranging 50 and 100, and inclination angles of 30°, 50° and 90° respectively. The results explain that the flow field is dominated by one cell rotating in a clockwise direction and filling the cavity. Also, the variation of the average Nusselt number with inclination angles is also presented. The results showed a good agreement with other published results.

التخمين العددي لظاهرة الحمل الحر خلال فجوة مائلة مستطيلة الشكل مملوءة بوسط مسامي.

د. أحمد كاظم حسين / مدرس
قسم الهندسة الميكانيكية – كلية الهندسة – جامعة بابل

داخلي طباقى متساوي الحرارة فوق فجوة مسامية مائلة مستطيلة الشكل. في هذا البحث تم استخدام موديل دارسي و المعادلات الحاكمة تم حلها بواسطة طريقة تحت التراخي. خواص الجريان تم حسابها لرقم براندل يساوي 0.7 والنسبة الباعية تساوي 1.5. الدراسة الحالية تضمنت إجراء الحسابات لقيم رقم رايلي 50 و 100 ولزاوية ميلان الفجوة بقيم 30° , 50° , 90° . النتائج أوضحت بأن الجريان يمثل بدوامة واحدة تدور باتجاه عقارب الساعة وتملئ الفجوة بأكملها. كذلك تم عرض نتائج التغير بين رقم نسلت المتوسط مع زوايا الميلان. النتائج أوضحت تطابق جيد مع النتائج الأخرى المنشورة.

Key words: Free convection , CFD , Cavity , Porous Media , Laminar Flow.

2. Nomenclature:

Symbol	Description	Dimension
A_s	The cavity aspect ratio = H / W	
c_p	Specific heat at constant pressure.	$KJ / kg \cdot ^\circ C$
g	Gravitational acceleration.	m/s^2
H	Cavity height.	m
K	The permeability of the porous media	m^2
k_e	Effective thermal conductivity of the porous media .	$W/m \cdot ^\circ C$
Nu_{av}	Average Nusselt number.	
P	Dimensionless pressure.	
p	pressure.	N/m^2
P_r	Prandtl number.	
Ra_w	Darcy-modified Rayleigh number based on the cavity width (W).	
r	Under-Relaxation parameter (usually less than unity)	
T	Temperature.	$^\circ C$
u	Velocity component in x-direction.	m/s
v	Velocity component in y-direction.	m/s
W	Cavity width	m
X	Dimensionless Coordinate in horizontal direction.	
x	Coordinate in horizontal direction.	m
Y	Dimensionless Coordinate in vertical direction.	
y	Coordinate in vertical direction.	m

Greek Symbols

α_e	Effective thermal diffusivity of the porous	m^2/s
------------	---	---------

	media.	
β	Volumetric coefficient of thermal expansion.	K^{-1}
θ	Dimensionless temperature.	
μ	Dynamic viscosity of the fluid.	$N.sec/ m^2$
ν	Kinematic viscosity of the fluid.	m^2/s
ρ	Density of the fluid.	Kg/m^3
Ψ	Stream function.	m^2/s
Ψ_D	Dimensionless stream function.	
Φ	Angle of inclination.	Degree
$\Delta X, \Delta Y$	Dimensionless spatial steps in computational domain.	
$\Delta x, \Delta y$	spatial steps in computational domain.	m

Subscript

- c Cold
- f Fluid
- h Hot

i, j Node symbols indicates position in x and y directions respectively.
w Conditions at surface.

3.Introduction : Free convection flows in a porous media occurs in a number of important practical situations such as in an air-saturated fibrous insulation material surrounding a heated body, heat transfer from a pipe or a cable buried in a soil , flow in an oil reservoir in a geothermal power system, at some building applications in which heat is transferred across an insulation-filled cavity and about pipes buried in water-saturated soils. These are just some examples for engineering applications where basically a cavity filled with a porous media **Oztop** (2007) and **Varol et al.** (2006). The porous media consists of a bed of many relatively closely packed particles or some other form of solid matrix which remains at rest and through which a fluid flows. Natural or free convection in a porous media has been studied in recent years. **Cheng** (1974) provided a comprehensive review of the literature on free convection in a porous media with a focus on geothermal systems. **Prakash et al.**(1999) presented a model to predict heat and mass transfer in a system consisting of a turbulent flow overlying a saturated hygroscopic porous medium. They concluded that for large enclosures the flow was turbulent due to high Rayleigh numbers and in the porous

media the turbulence was not important if the system has a sufficiently low permeability. **Al-Amiri** (2000) performed a numerical studies of momentum and energy transfer in a lid-driven enclosure filled with a saturated porous medium. In his study, the force convection is induced by sliding the top constant temperature wall. It was found that the increase in Darcy number induces flow activities causing an increase in the fraction of energy transport by means of convection. **Khanfer** and **Vafai** (2002) extended the previous work of **Al-Amiri** (2000) to mass transport in the media. The buoyancy effects that create the flow are induced by both temperature and concentration gradients. They concluded that the influences of the Darcy number and buoyancy ratio on thermal and flow were significant. **Al-Bahi et al.** (2002) studied numerically laminar natural convection heat transfer in an air filled vertical square cavity differentially heated with a single isoflux discrete heater on one wall with top and bottom adiabatic surfaces. Numerical results indicated that the local Nusselt number decreases along the length of the heater at constant value of modified Rayleigh number. **Al-Nimr** and **Khadrawi** (2003) investigated the problem of transient free convection in domains partly filled with porous substrates analytically using Laplace transformation technique. Four configurations were considered which are subject to an isothermal heating boundary condition. The Brinkman-extended Darcy model was adopted to describe the hydrodynamics behavior of the porous domain. **Pakdee** and **Rattanadecho** (2005) made a parametric study for natural convective flow in a fluid-saturated porous medium in a square cavity. The top surface is partially open to the ambient allowing the surface temperature to change depending on the influence of convection heat transfer mechanism. The governing equations were solved by the standard Gauss-Seidel line relaxation procedure. In the current work, a numerical simulation gives the results with a short-time and an accurate computation and the computer program may be changed easily to deal with any other complex shapes such as enclosures, sphere and circular ducts. In the numerical simulation, the governing differential equations are solved by replacing it with differences, calculated from a finite number of values associated with the computational nodes, which are distributed on a suitable grid over the solution domain. In the present study, the Under-Relaxation explicit technique is adopted to predict the free convection characteristics of two-dimensional internal laminar isothermal flow over an inclined rectangular porous cavity to predict the temperature and the stream function variations on the free convection for

different range of Rayleigh number and inclination angles of the cavity. In the next section, the mathematical analysis will be given in detail and the procedure, which used to solve the governing equations was described.

4. Mathematical Analysis: The studied case is a rectangular porous media –filled cavity which is inclined at an angle Φ to the vertical. One wall of the cavity is kept at a uniform hot temperature (T_h) and the other wall is kept at a uniform cold temperature (T_c). The other two walls of the cavity are assumed to be adiabatic (i.e, it is assumed that no heat is transferred into or out of these walls). The configuration under consideration is shown schematically in Fig. (1). The rectangular cavity has a height (H) and width (W) and the working fluid is chosen as air with Prandtl number $P_r = 0.7$. The flow described by **continuity, momentum and energy equations**. These equations are written in a dimensionless form by dividing all dependent and independent variables by suitable constant terms.

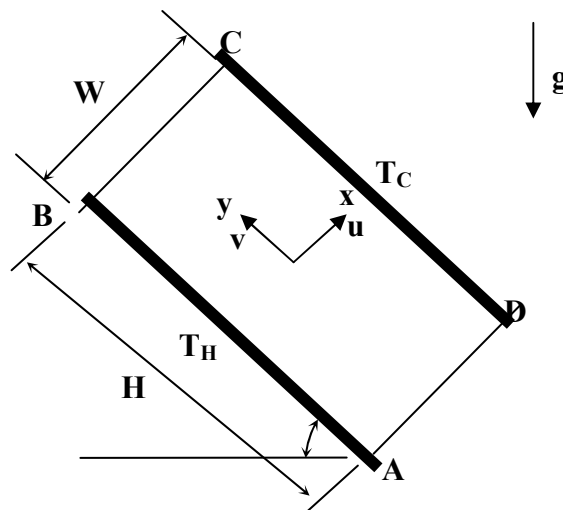


Fig.1

The solution is obtained using Under-Relaxation finite difference scheme and the following assumptions are considered :-

1. The fluid velocity over the particle is small and the Reynolds number based on the particle size will be very small , so the flow over the particles will be a Stokes type flow.

2. The size of the particles considered is small compared to the overall size of the system.
3. The flow is considered steady , two-dimensional.
4. The fluid and the porous media are assumed to be in local thermal equilibrium.
5. The fluid and porous media properties are assumed to be constant.
6. Darcy model of flow is assumed which states that the flow velocities are low and that the momentum changes and viscous forces in the fluid are consequently negligible compared to the drag force and buoyancy force.
7. The fluid inside the cavity is assumed Newtonian and the density variations are related only to the buoyancy terms of the momentum equations (Boussinesq approximation) .
8. The temperature of the fluid phase is equal to the temperature of the solid phase every where in the porous media.

The governing equations for a two-dimensional, steady, laminar flow expressed in conservation form are

Continuity equation:

$$\frac{\partial u}{\partial x} + \frac{\partial v}{\partial y} = 0 \quad , \quad \dots(1)$$

Momentum equations:

$$\frac{\mu_f u}{K} = -\frac{\partial p}{\partial x} + \beta g \rho_f (T - T_c) \cos \Phi \quad \dots(2-a)$$

$$\frac{\mu_f v}{K} = -\frac{\partial p}{\partial y} + \beta g \rho_f (T - T_c) \sin \Phi \quad \dots(2-b)$$

Energy equation :

$$u \frac{\partial T}{\partial x} + v \frac{\partial T}{\partial y} = \alpha_e \left(\frac{\partial^2 T}{\partial x^2} + \frac{\partial^2 T}{\partial y^2} \right) \quad \dots(3)$$

The cold wall temperature (T_c) has been taken as the reference temperature. The solution will be obtained in terms of the stream function which is defined by **White** (1996):

$$u = \frac{\partial \Psi}{\partial y} \text{ and } v = -\frac{\partial \Psi}{\partial x} \quad \dots(4)$$

The magnitude of the stream function is a measure of the strength of the fluid motion in the cavity. Now, if the pressure (p) is eliminated by taking the y-derivative of **Eq.(2-a)** and the x-derivative of **Eq.(2-b)** and the two equations are subtracted so the result gives:

$$\frac{\mu_f}{K} \left(\frac{\partial u}{\partial y} - \frac{\partial v}{\partial x} \right) = \beta g \rho_f \left(\frac{\partial T}{\partial y} \cos \Phi - \frac{\partial T}{\partial x} \sin \Phi \right) \quad \dots(5-a)$$

Now, by using the definition of the stream function (**Eq.(4)**) yields:

$$\left(\frac{\partial^2 \Psi}{\partial y^2} + \frac{\partial^2 \Psi}{\partial x^2} \right) = \frac{\beta g \rho_f K}{\mu_f} \left(\frac{\partial T}{\partial y} \cos \Phi - \frac{\partial T}{\partial x} \sin \Phi \right) \quad \dots(5-b)$$

Also, in terms of the stream function (**Eq.(4)**), the energy equation (**Eq.(3)**) becomes

$$\frac{\partial \Psi}{\partial y} \frac{\partial T}{\partial x} - \frac{\partial \Psi}{\partial x} \frac{\partial T}{\partial y} = \alpha_e \left(\frac{\partial^2 T}{\partial x^2} + \frac{\partial^2 T}{\partial y^2} \right) \quad \dots(6)$$

The effective thermal diffusivity (α_e) is not the thermal diffusivity of the fluid, since it is the ratio of the effective thermal conductivity of the porous media to the product of the density and the specific heat at constant pressure of the fluid (i.e, $\alpha_e = \frac{k_e}{\rho c_p}$). In

order to put these equations in the dimensionless form, the following dimensionless variables are used:-

$$X = x / W, \quad Y = y / W, \quad \Psi_D = \frac{\Psi}{\alpha_e} \quad \text{and} \quad \theta = \frac{T - T_c}{T_h - T_c}$$

In terms of these dimensionless variables **Eqs.(5-b)** and **(6)** become:

$$\left(\frac{\partial^2 \Psi_D}{\partial X^2} + \frac{\partial^2 \Psi_D}{\partial Y^2} \right) = Ra_w \left(\frac{\partial \theta}{\partial Y} \cos \Phi - \frac{\partial \theta}{\partial X} \sin \Phi \right) \quad \dots(7)$$

$$\frac{\partial \Psi_D}{\partial Y} \frac{\partial \theta}{\partial X} - \frac{\partial \Psi_D}{\partial X} \frac{\partial \theta}{\partial Y} = \left(\frac{\partial^2 \theta}{\partial X^2} + \frac{\partial^2 \theta}{\partial Y^2} \right) \quad \dots(8)$$

where Ra_w is the Darcy-modified Rayleigh number based on the cavity width (W) which is defined by **Nield** and **Bejan** (2006) as :-

$$Ra_w = \frac{\beta g K (T_h - T_c) W}{\alpha_e \nu_f}$$

The rate of heat transfer is expressed in terms of average Nusselt number (Nu_{av}) as follows :

$$Nu_{av} = \int_0^1 \left[\frac{\partial \theta}{\partial X} \right]_{X=0} dY \quad \dots(9)$$

Boundary conditions

The boundary conditions which are used in the present study can be arranged as follows:-

1. Velocity components normal to the wall equals zero, so:

$$u = v = 0.0 \quad \text{at } x = 0 \quad \text{and } x = W \quad \text{for } 0 \leq y \leq H$$

$$u = v = 0.0 \quad \text{at } y = 0 \quad \text{and } y = H \quad \text{for } 0 \leq x \leq W$$

2. The top and bottom walls are thermally insulated, so:

$$\frac{\partial T}{\partial y} = 0 \quad \text{at } y = 0 \quad \text{and } y = H$$

In terms of the stream function, this means that:

$$\frac{\partial \Psi}{\partial y} = 0 \quad \text{at } x = 0 \quad \text{and } x = W$$

$$\frac{\partial \Psi}{\partial x} = 0 \quad \text{at } y = 0 \quad \text{and } y = H$$

3. The left and right walls are maintained at isothermal hot and cold temperatures respectively, so:

$$T = T_h \quad \text{at } x = 0 \quad \text{and} \quad T = T_c \quad \text{at } x = W$$

4. At all wall surfaces

$$\Psi = 0.0$$

In terms of the above dimensionless variables, the boundary conditions become :-

$$\text{at } X = 0.0 \quad \theta = 1.0$$

$$\text{at } X = 1.0 \quad \theta = 0.0$$

$$\text{and at all the walls} \quad \Psi_D = 0.0$$

$$\text{at } Y = 0.0 \quad \frac{\partial \theta}{\partial Y} = 0$$

$$\text{at } Y = A_s \quad \frac{\partial \theta}{\partial Y} = 0$$

5.Numerical Analysis: Explicit Under-Relaxation space-marching finite difference method is used to solve the set of governing equations [Eq.(7) and Eq.(8)]. By using this technique a computer code is developed to predict the stream function and temperature .The details are follows :-

5.1 Dimensionless Governing Equations in a Discretized Form:

a. Dimensionless Stream Function.

$$\Psi_{D i, j} = \left\{ \left[\frac{\Psi_{D i+1, j} + \Psi_{D i-1, j}}{\Delta X^2} \right] + \left[\frac{\Psi_{D i, j+1} + \Psi_{D i, j-1}}{\Delta Y^2} \right] - Ra_w \left(\left[\frac{\theta_{i, j+1} - \theta_{i, j-1}}{2 \Delta Y} \right] \cos \Phi - \left[\frac{\theta_{i+1, j} - \theta_{i-1, j}}{2 \Delta X} \right] \sin \Phi \right) \right\} / \left[\frac{2}{\Delta X^2} + \frac{2}{\Delta Y^2} \right] \quad \dots(10)$$

Eq.(10) can be calculated using Under-Relaxation scheme so that :-

$$\Psi_{D i, j}^1 = \Psi_{D i, j}^0 + r(\Psi_{D i, j}^{calc} - \Psi_{D i, j}^0) \quad \dots(11)$$

b. Dimensionless Temperature.

$$\theta_{i, j} = \left\{ \left[\frac{\theta_{i+1, j} + \theta_{i-1, j}}{\Delta X^2} \right] + \left[\frac{\theta_{i, j+1} + \theta_{i, j-1}}{\Delta Y^2} \right] - \left[\frac{\Psi_{D i, j+1} - \Psi_{D i, j-1}}{2 \Delta Y} \right] \left[\frac{\theta_{i+1, j} - \theta_{i-1, j}}{2 \Delta X} \right] + \left[\frac{\Psi_{D i+1, j} - \Psi_{D i-1, j}}{2 \Delta X} \right] \left[\frac{\theta_{i, j+1} - \theta_{i, j-1}}{2 \Delta Y} \right] \right\} / \left[\frac{2}{\Delta X^2} + \frac{2}{\Delta Y^2} \right] \quad \dots(12)$$

Again Eq.(12) can be calculated using Under-Relaxation scheme so that :-

$$\theta_{i, j}^1 = \theta_{i, j}^0 + r(\theta_{i, j}^{calc} - \theta_{i, j}^0) \quad \dots(13)$$

where $\theta_{i, j}^{calc}$ is the value given by Eq.(12), $\theta_{i, j}^0$ is the value of $\theta_{i, j}$ at the previous iteration and

r is the Under-Relaxation parameter which is usually less than unity. Eq.(12) is applied at all internal nodes (i.e., at all points within the cavity). The use of an iterative solution method needs a convergence and stopping criteria to terminate the iteration process. To make the present solution stable and to obtain a reasonable accuracy, so that the computation is terminated when all of the residuals get below 10^{-5} .

6. Code Verification:

The numerical algorithm is tested by considering a square vertical porous cavity under the same boundary conditions but the numerical scheme is different which is studied by Oosthuizen and Naylor (1999) for aspect ratio = 1.0 and a Rayleigh number = 50. This problem is treated by the present numerical scheme in order to compare it with the previous work by Oosthuizen and Naylor (1999). In order to make the comparison applicable the angle of inclination is taken as 90° (Vertical Cavity). The comparison between the stream function and temperature results are shown a good agreement between the present and the previous schemes as shown in Fig.(2) and Fig.(3) respectively.

7. Results and Discussion:

Figure (4) shows the evolution of the flow and thermal fields in the cavity when $Ra = 50$, aspect ratio = **1.5** and angle of inclination = **30 degree**. It may be noted that the negative sign of stream function denotes the clockwise circulation. The non-slip condition is valid at all boundaries as there is no cross-flow, hence $\Psi = 0.0$ is used for the boundaries. It is interesting to note that, the higher values of stream function means higher flow rate. As is clear from this figure, convective vortices or rolls are observed. Also, in this figure the isotherms are observed to be a uniform lines. As expected due to the heated left vertical wall, fluid rise up along the side of left wall and flow down along the cooled right wall forming a usual convective roll or circulation with clockwise rotation inside the cavity. It can be observed that, the flow circulation inside the cavity is greater near the center and least near the wall due to no slip boundary conditions.

Figure (5) and **Figure (6)** illustrate the dimensionless stream function and dimensionless temperature contours in the cavity when $Ra = 50$, aspect ratio = **1.5** and angle of inclination = **50** and **90** degrees respectively. As seen from these figures the temperature contours are smooth curves which covers the entire cavity. These figures also show the presence of significant effect of free convection on temperature contours which start getting deformed and pushed towards the side wall. The figures show that the existence of strong circulation causes a good fluid mixing process in the cavity. This increase in the heat flux is due to the increase in the velocity also the other reason of this increasing is due to buoyancy forces which causes an increase in the mass flow rate close to the wall and accelerate the fluid flow so as a result causes an increasing in the amount of the heat flux. It is observed from these figures that the intensity of circulation increases with increasing the angle of inclination. Also, the greater circulation causes more heat to be distributed in the central region of the cavity.

In **Figure (7)** the dimensionless stream function and isotherm contours in the cavity are displayed when $Ra = 100$, aspect ratio = **1.5** and angle of inclination = **30** degree. In this figure, the circulation patterns of the flow field are also noticed. The heated portions of the fluid become lighter than the rest of the fluid, and are exposed laterally away from the center to the sides, then flow down along the two vertical walls, leading to the clockwise flow circulations. These results suggest that the buoyancy forces are able to overcome the influence of viscous forces. Also this figure shows that the number of

convective vortices or cells and the circulation intensity increases with increasing Rayleigh number .

The evolution of the flow and thermal fields when $Ra = 100$, for a cavity of aspect ratio = 1.5 for a representative case with angle of inclination = 50 and 90 degrees respectively are presented in **Figure (8)** and **Figure (9)** respectively. The flow pattern is characterized by a convection roll with clockwise rotation inside the cavity. Again a stronger circulation occurs when a Rayleigh number increases. The circulations are greater near the center and least at the wall due to no-slip boundary conditions. As shown in these figures, the hot fluid rises in the central region as a result of buoyancy forces, and then it moves downwards along the vertical walls and turns horizontally to the central region after hitting the bottom wall. However, in the convection region adjacent to the heat source, the isotherms become thinner producing higher temperature gradients. It is observed that for vertical cavity ($\Phi = 90^\circ$), as shown in **Fig.(2)** the buoyancy force is acting only in one direction, while for the inclined cavity the buoyancy force components acting in both x and y directions. The effect of cavity inclination is clearly visible on both the flow patterns and isotherms as shown in **Fig.(9)**. Moreover from these figures it is observed from isotherms that as Rayleigh number increases, the temperature gradients in lower corners of the cavity increases, thus increasing the heat transfer in this region. **Figures (10)** and **(11)** show the variation of the average Nusselt number with inclination angles for a rectangular inclined cavity when $Ra = 50$ and $Ra = 100$ respectively. It is seen from these figures that the average Nusselt number increases when the values of inclination angles increase. The heat transfer rate reaches a maximum value when the inclination angle is about 50 degree and then decreases as seen from **Figure (11)**. At this angle, the flow along both the heated wall and the adiabatic top wall is acted by buoyancy forces that are parallel to the wall. Also, these figures indicate that the average Nusselt number increases when the values of Rayleigh number increases.

8. Conclusions:

The following conclusions can be drawn from the results of the present work :-

1. It is observed that the intensity of circulation increases with increasing the angle of inclination .Also, the greater circulation causes more heat to be distributed in the central region of the cavity.

2. The vortices (or convection currents) are formed and a higher fluid circulation is found in the flow domain due to stronger free convection effects.
3. The number of convective vortices or cells increases with increasing Rayleigh number .
4. From an examination of the isotherms (dimensionless temperature lines) ,it is observed that for small values of Rayleigh number, convective motion is first observed near the lower corners of the cavity. As Rayleigh number increases, the temperature gradients in this region increases , thus increasing the heat transfer in this region.
5. From the stream line plots, it can be seen that the value of stream function (i.e., the flow rate) increases with increasing Rayleigh number.
6. Stronger circulation occurs at higher Rayleigh number. The circulations are greater near the center and least at the wall due to no-slip boundary conditions.
7. At the small Rayleigh number, the stream functions are almost circular. As Rayleigh number increases, the buoyancy driven circulation inside the cavity also increases as seen from greater magnitudes of the stream functions.
8. Due to stronger circulation at high Rayleigh number, the isotherms are largely compressed near the middle portion of the side vertical walls.
9. It is noted that as the value of the Rayleigh number increases, a finite and symmetric disturbance is imposed on the temperature field.
10. It can be concluded to an interesting note that not only an intensity of a flow, but also the direction of the fluid flow locally affects the heat convection process.
11. The average Nusselt number increases when the values of Rayleigh number and the inclination angle increase.

9. Referencers .

Oztop , H. "Natural Convection in Partially Cooled and Inclined Porous Rectangular Enclosures", International Journal of Thermal Sciences, Vol.46, 2007 , pp: 149- 156.

Varol, Y., Oztop, H. and Varol, A., "Free Convection in Porous Media Filled Right-Angle Triangular Enclosures", International Communications in Heat and Mass Transfer, Vol.33, 2006, pp: 1190-1197.

Cheng, P. "Heat Transfer in Geothermal Systems", Advances in Heat Transfer, Vol.4, 1978, pp: 1-105.

Al-Amiri, A. "Analysis of Momentum and Energy in a lid-driven Cavity Filled with a Porous Medium", International Journal of Heat and Mass Transfer, Vol.43, 2000, pp: 3513-3527.

Khanafar, K. and Vafai, K. "Double Diffusive Mixed Convection in a Lid Driven Enclosure Filled with a Fluid - Saturated Porous Medium", Numerical Heat Transfer, Part A, Vol.42, 2002, pp: 465-486.

Al-Bahi, A., Radhwan, A. and Zaki, G. "Laminar Natural Convection From an IsoFlux Discrete Heater in a Vertical Cavity", Arabian Journal for Science and Engineering, Vol.27, No.2 C, 2002, pp: 149-164.

Al-Nimr, M. and Khadrawi, A. "Transient Free Convection Fluid Flow in Domains Partially Filled with Porous Media", Transport in Porous Media, Vol.51, No.2, 2003, pp: 157-172.

Pakdee, W. and Rattanadecho, P. "Natural Convective Heat Transfer Through Porous Media in Cavity Due to Top Surface Convection", The 19th Conference of Mechanical Engineering Network of Thailand, 19-21 October, 2005, Phuket, Thailand.

White, F. "Fluid Mechanics", Fourth Edition, McGraw-Hill Series in Mechanical Engineering, U.S.A., 1996.

Nield, D. and Bejan, A. "Convection in Porous Media", Third Edition, Springer Publications, 2006.

Oosthuizen, P. and Naylor, D. "Introduction to convective Heat Transfer Analysis", McGraw-Hill Company, U.S.A., 1999.

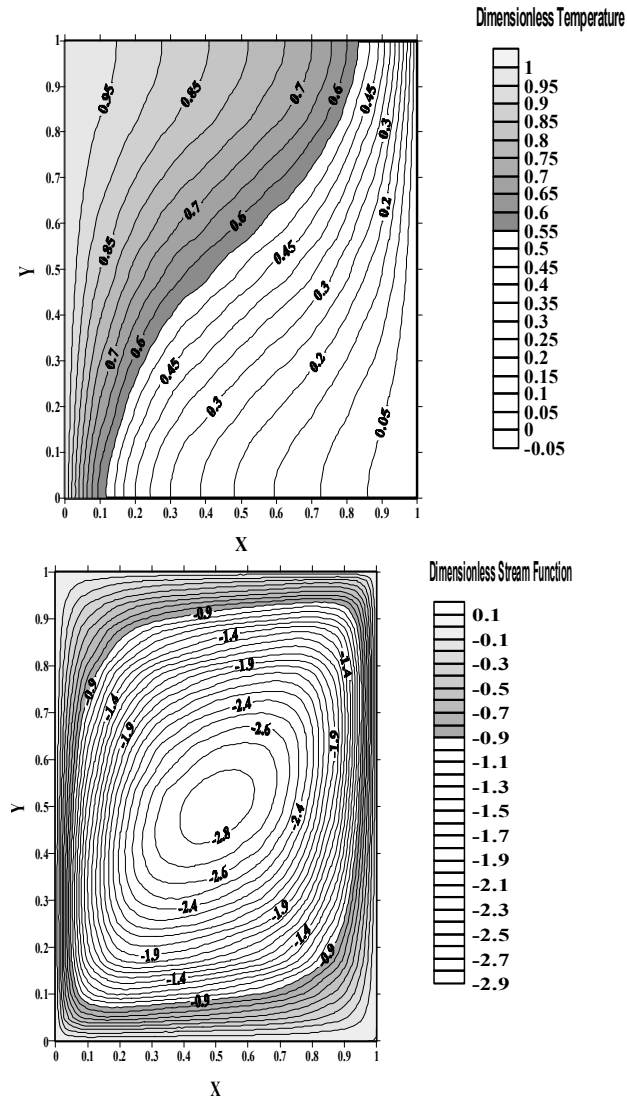


Fig. (2)Dimensionless stream function (right) and dimensionless temperature (left) contours for a square cavity when $Ra = 50$, Aspect ratio = 1.0 and angle of inclination = 90 degree (Present scheme).

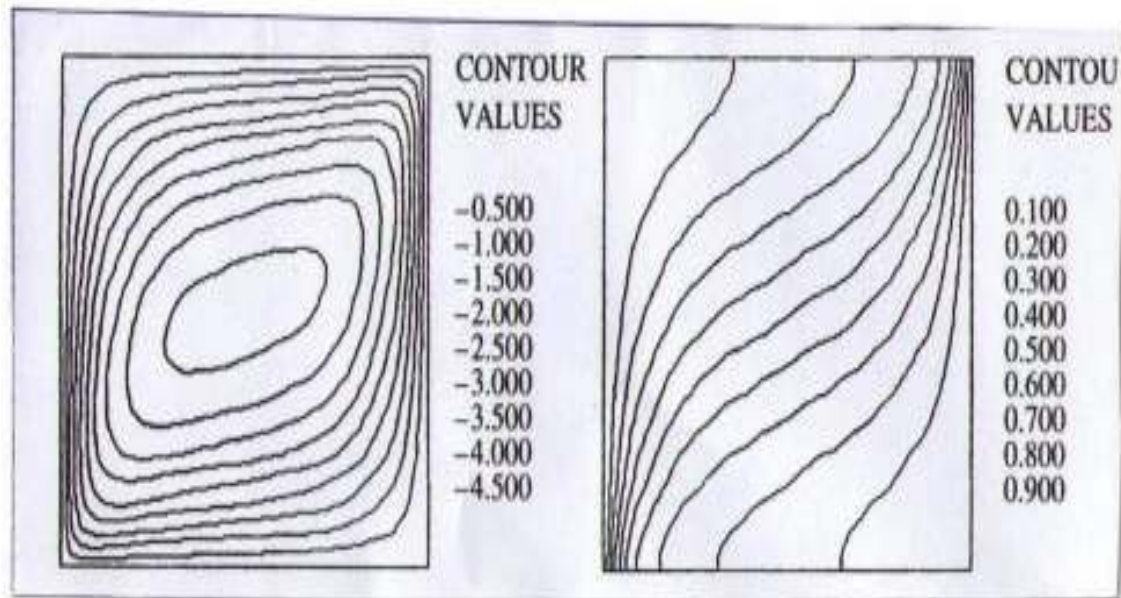
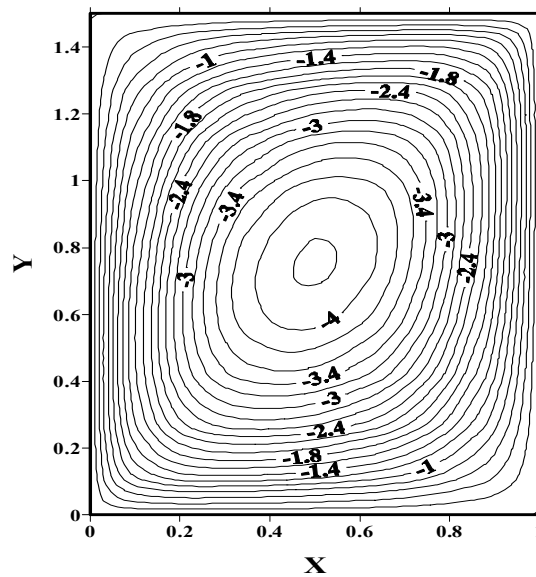


Fig. (3) Dimensionless stream function (left) and dimensionless temperature (right) contours for a square cavity when $Ra = 50$, Aspect ratio = 1.0 and angle of inclination = 90 degree (Oosthuizen and Naylor (1999) scheme).



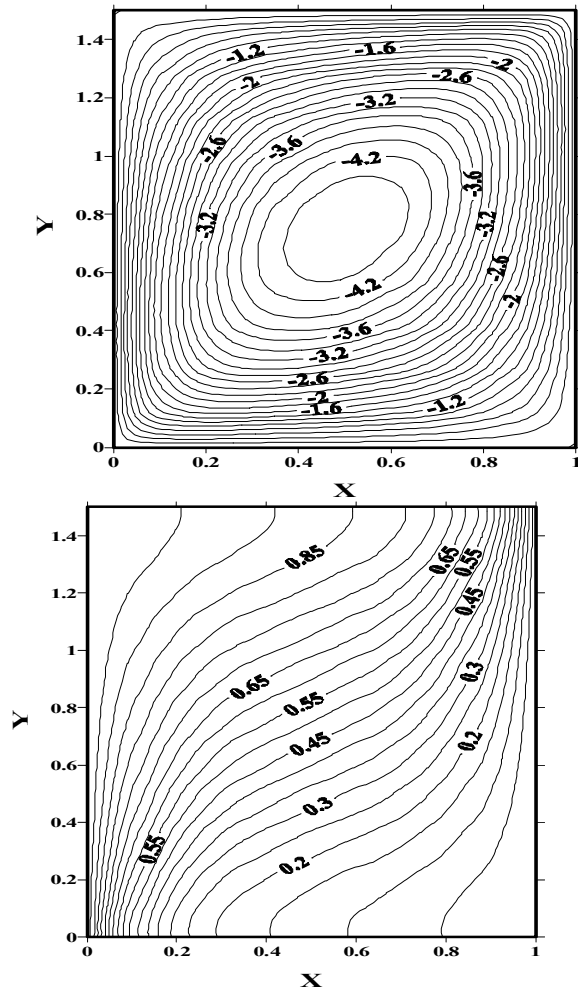


Fig. (5) Dimensionless Stream function (right)and temperature (left)contours for a rectangular cavity when $Ra = 50$, Aspect ratio = 1.5 and angle of inclination = 50 degree.

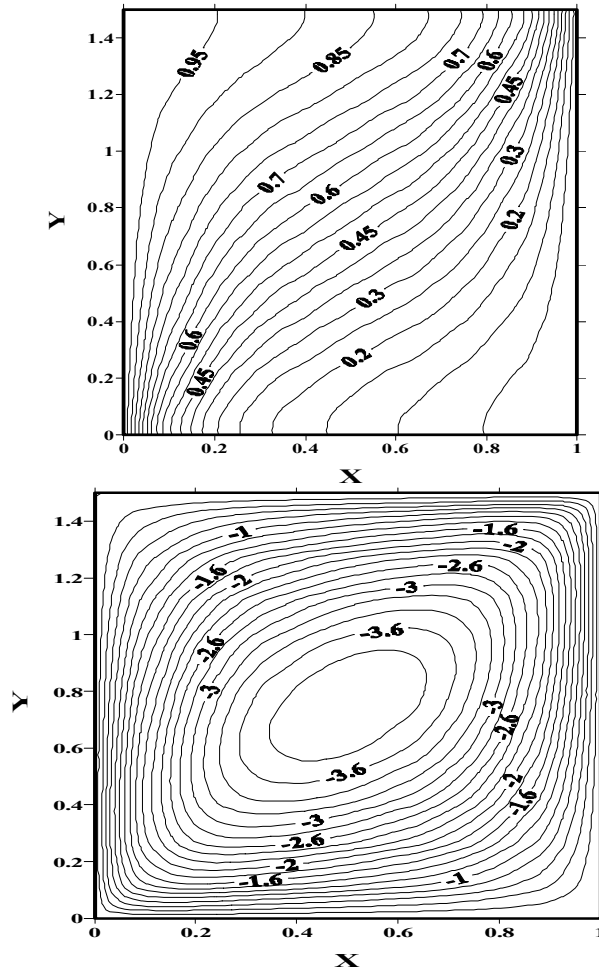


Fig. (6) Dimensionless Stream function (right) and temperature (left) contours for a rectangular cavity when $Ra = 50$, Aspect ratio = 1.5 and angle of inclination = 90 degree.

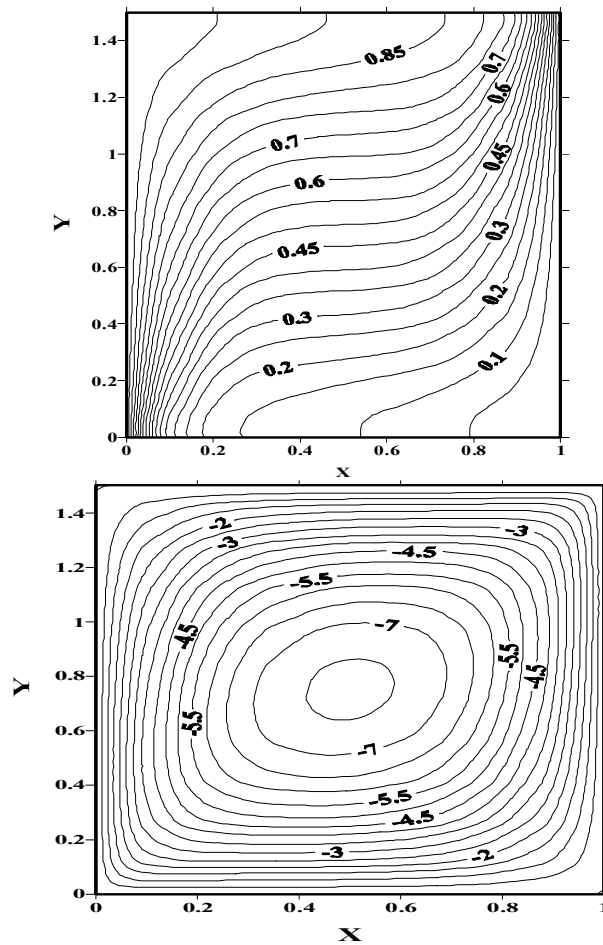


Fig. (7) Stream function (right) and temperature (left) contours for a rectangular cavity when $Ra = 100$, Aspect ratio = 1.5 and angle of inclination = 30 degree.

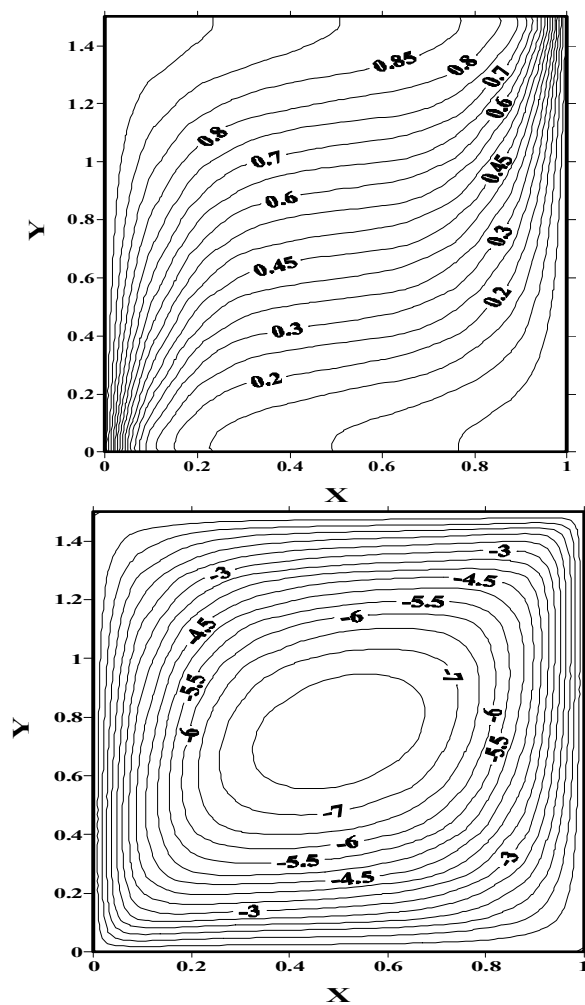


Fig. (8) Stream function (right) and temperature (left) contours for a rectangular cavity when $Ra = 100$, Aspect ratio = 1.5 and angle of inclination = 50 degree.

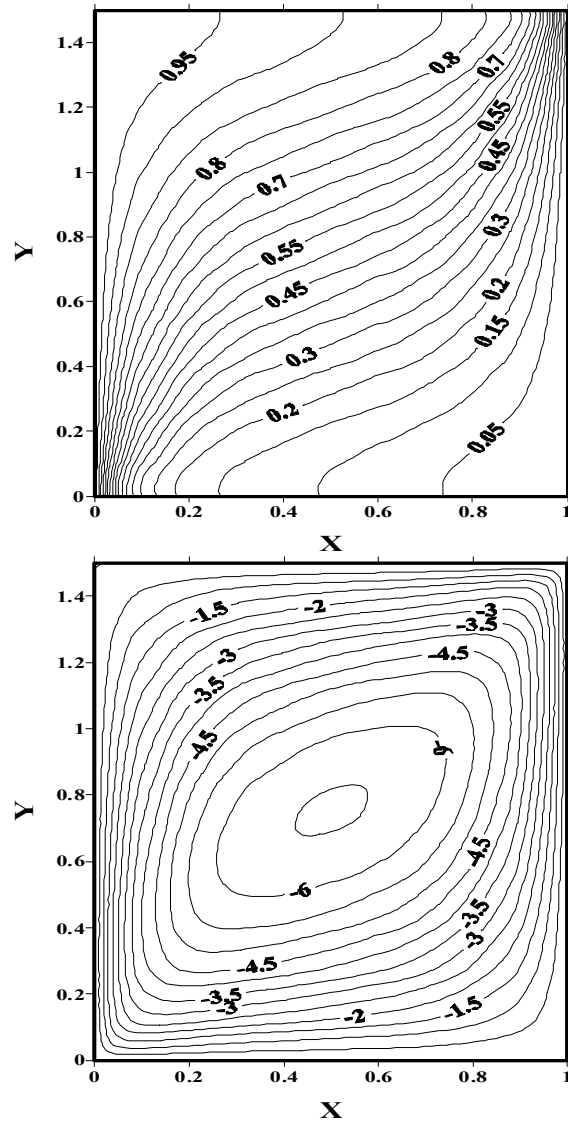


Fig. (9) Stream function (right) and temperature (left) contours for a rectangular cavity when $Ra = 100$, Aspect ratio = 1.5 and angle of inclination = 90 degree.

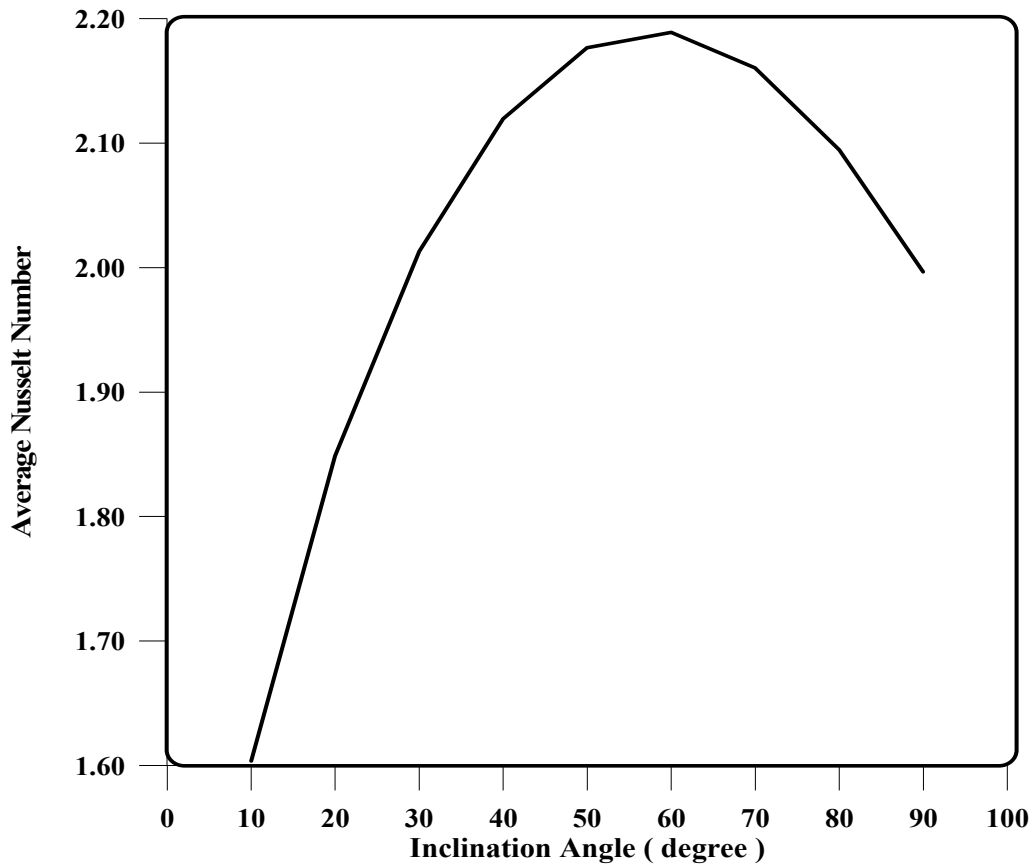


Fig. (10) Variation of the average Nusselt number with inclination angles for a rectangular cavity when $Ra = 50$, Aspect ratio = 1.5 .

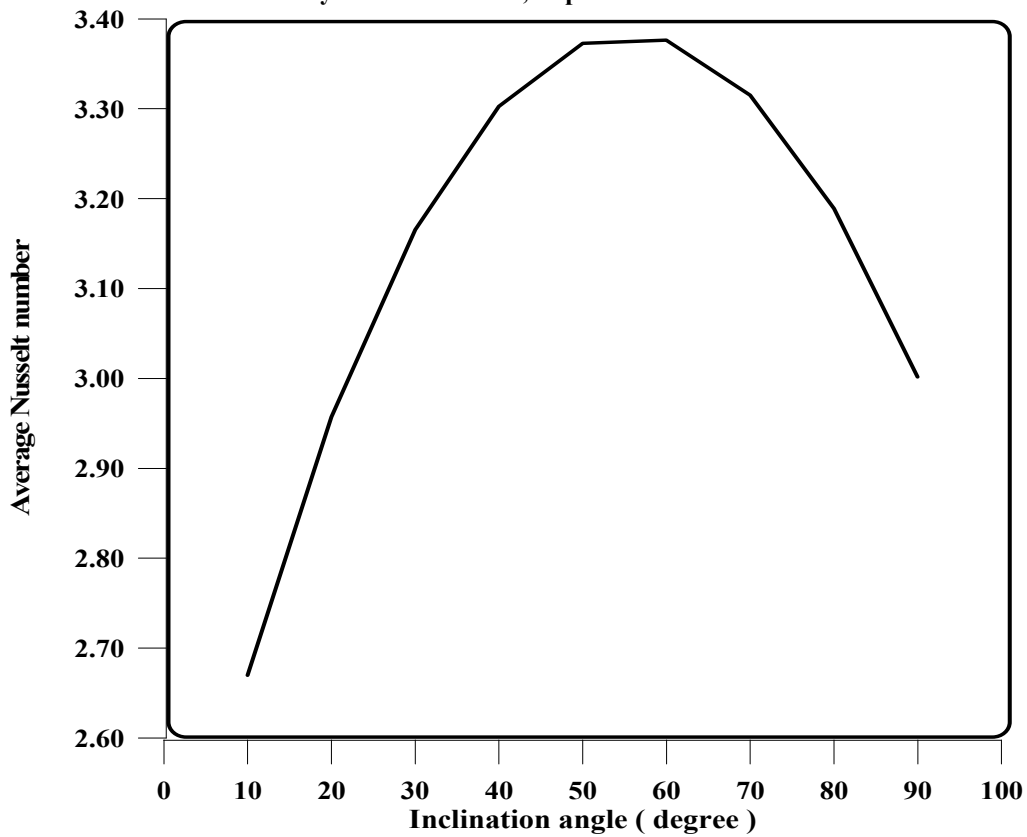


Fig. (11) Variation of the average Nusselt number with inclination angles for a rectangular cavity when $Ra = 100$, Aspect ratio = 1.5 .